Modeling individual fear factor with optimal control in a disease-dynamic system

Article *in* Chaos Solitons & Fractals · November 2017

DOI: 10.1016/j.chaos.2017.09.001

CITATIONS
4

READS
162

5 authors, including:

Yuyang Chen
Kansas State University
7 PUBLICATIONS **7** CITATIONS
SEE PROFILE

Kaiming Bi
Kansas State University
9 PUBLICATIONS **28** CITATIONS
SEE PROFILE

Songnian Zhao
Kansas State University
18 PUBLICATIONS **46** CITATIONS
SEE PROFILE

David Ben-Arieh
Kansas State University
124 PUBLICATIONS **1,703** CITATIONS
SEE PROFILE

Chaos, Solitons and Fractals 104 (2017) 531–545

Contents lists available at ScienceDirect

Chaos, Solitons and Fractals

Nonlinear Science, and Nonequilibrium and Complex Phenomena

journal homepage: www.elsevier.com/locate/chaos

Modeling individual fear factor with optimal control in a disease-dynamic system

Yuyang Chen, Kaiming Bi, Songnian Zhao, David Ben-Arieh, Chih-Hang John Wu*

Department of Industrial & Manufacturing Systems Engineering, Kansas State University, 1701B Platt St., Manhattan, KS 66502, USA

ARTICLE INFO

Article history:
Received 10 February 2017
Revised 1 September 2017
Accepted 4 September 2017

Keywords:
Individual fear factor
Disease dynamic
Behavior change
Stability analysis
Optimal control

ABSTRACT

This paper proposes a new, information-transmission-based behavior-switch that applies the individual fear factor (IFF) to describe how information regarding current disease epidemics can cause human behavior change in a disease-dynamic system. This research is a first attempt to mathematically model how an individual's emotions influence behavior. The approach can be used to study the relationship of information dissemination (e.g., broadcasting, public health education, news media, etc.) and human behaviors during disease outbreaks. The expression of IFF and a mathematical IFF model that combines human behaviors with a classic SIR model is presented, and an optimal strategy that reduces the number of infected individuals and financial loss due to switch behaviors is proposed. In particular, model stability is analyzed and corresponding necessary conditions are determined. This novel modeling approach shows that information transmission influence individual fear, resulting in a variety of human behaviors and leading to numerous disease consequences.

Published by Elsevier Ltd.

1. Introduction

Human behavior changes throughout an infectious disease epidemic have recently been identified as a dominating factor in epidemics and have attracted considerable attention in the literature [1–4]. Increased understanding of the interconnectedness of human behavior changes and the underlying epidemic could help governments and public health agencies develop more effective protective measures and mitigation strategies. Because individuals receive disease information from various sources, e.g., news broadcast, social media contacts, updated prevalence on a disease, etc., each person may exhibit unique behaviors, such as utilization of protective masks, vaccination, social distancing, self-quarantine, or other self-protections to reduce the chances of infection. On the other hand, individuals may refuse to implement protective measures because they think the measures could be inconvenient or expensive. These unique, spontaneous behavior patterns based on diverse knowledge or opinions derived from similar information may lead to a variety of disease epidemic results; therefore, the primary objective of this article is to model and study human behavior changes and subsequent impacts on the underlying disease epidemic.

During an epidemic outbreak, individuals may possess distinctive viewpoints on and responses to long-term disease risks. Lemerise and Arsenio [5] found that social information can influences emotional and cognitive processes. Similar research discovered that human emotion can be formed based on the information acquired [6], and Shiota and coworkers [7] determined that emotions are unique. Zhao et al. [8] used a spatial evolutionary game to investigate how prevalence information in a disease can influence human behaviors. In 2010 Funk et al. [1] reviewed current human behavior models and researched the impact of human behavior on infectious disease dynamics. Johnston and Warkentin [9] identified that fear, a common emotional expression of individuals during disease outbreaks, can initiate human protection motivation. In 1965 Geer [10] first proposed the concept and measure of the fear factor which is the result in external stimuli.

To the best of our knowledge, no research has investigated how disease information result in human opinion and emotion then how to act on human behaviors throughout a disease epidemic. Public health agencies are often unable to fully control spontaneous changes of human behavior during an epidemic because, although individuals may receive similar information regarding a disease, each individual uniquely interprets the knowledge and forms distinctive opinions that affect his or her decisions and behavior. Actually, in 2009 Funk et al. [11] proposed the spread of awareness could affect the spread of disease, although it could not stop the disease, it can lower the infection rate significantly. Their paper considered the awareness just can spread through the media

* Corresponding author.
E-mail addresses: cyy@ksu.edu (Y. Chen), bikaiming@ksu.edu (K. Bi), songnian@ksu.edu (S. Zhao), davidbe@ksu.edu (D. Ben-Arieh), chw@ksu.edu (C.-H.J. Wu).

http://dx.doi.org/10.1016/j.chaos.2017.09.001
0960-0779/Published by Elsevier Ltd.

which is the information disseminated in global, and they provided some analysis to support the impact of spread of awareness on epidemic. The difference of ideas between their paper and this paper is that their paper proposed the spread of awareness could influence the spread of disease because it is related to the infection rate. However, the idea of this paper is that propose the mathematical definition of individual fear factor and consider individual fear factor can change human behavior, which is not considered in their paper. In this paper we mathematically model the individual fear factor (IFF) and analyze its connection to epidemic information and spontaneous human behavior. Our study of IFF is based on the perceptual and rational aspects of information, considering local and global information. We also propose an expression of individual fear factor in three different parts: inertia part, perceptual part, and rational part. The inertia aspect of information indicates the impact of one's IFF on the next IFF for all individuals. For the perceptual aspect of information, our model considers how emotions from in the population spread and affect the IFF of an individual, including unprecedented consideration of self-mood. The rational aspect of information reflects how official or objective data pertaining to the number of infected individuals and switched susceptible individuals effect IFF.

The primary objective of this paper is to demonstrate how IFF is connected to susceptible individuals' changes in human behavior during a disease epidemic. Our aim is to increase model suitability for population over a contact network in which a disease can transmit over physical contacts and information can travel over social contacts. The proposed mathematical model incorporates IFF into the classic SIR model. First, we focus on the expression of individual fear based on various aspects of information sources, and then we adopt the particle swarm optimization (PSO) method to calculate IFF when an individual receives information regarding a disease epidemic. Second, we investigate how IFF affects changes in human behavior by analyzing how many individuals alter their current behaviors due to IFF and then inputting the number of switching susceptible individuals into the well-known SIR model. In order to precisely define the relationship between IFF and the SIR model, however, we use a multiple regression model to analyze numerical results of the regression model (IFF-SIR model). Third, stability analysis of the IFF model and IFF-SIR model is conducted using stability study and its related theories, including investigation of stability conditions. Assuming that corporate social performance of individuals can be controlled or manipulated, the optimal control strategy is used in our model to research how to effectively and economically decrease the number of infected individuals during the outbreak of disease. Our control policy is based on decreasing benefits (payoffs) due to switching behaviors and the number of infected individuals. Finally, we determine and present continuous control of optimal social reduction function with numerical simulations.

The paper is organized as follows. Section 2 describes construction of the IFF model and IFF-SIR dynamic systems model. Section 3 introduces the simulation strategy for the IFF model and regression analysis. Section 4 presents stability analysis for the IFF and IFF-SIR dynamic systems models and corresponding verification using simulation, and Section 5 includes discussion of the optimal control model and strategy of the IFF-SIR model as well as calculations for numerical solutions. Section 6 provides summary and discussion.

2. Mathematical model

2.1. Disease transmission

In this paper we use the SIR model first formulated by Reed and Frost in the 1920s [12] to describe disease transmission. The classic SIR model is a host-host transmission pathway [13]. In our SIR model we consider the disease-spreading process among N population in which each individual is in one of three states: susceptible, infected, or recovered. In addition, because some individuals in the real world are born or die over one time epoch, we add newborn individuals and remove dead individuals at a rate μ. In the real world individuals randomly contact individuals in other states, potentially becoming infected or infecting others at an average rate β. Infected individuals can choose measures to recover and acquire immunity, thereby guaranteeing they do not suffer from this disease at a recovery rate γ.

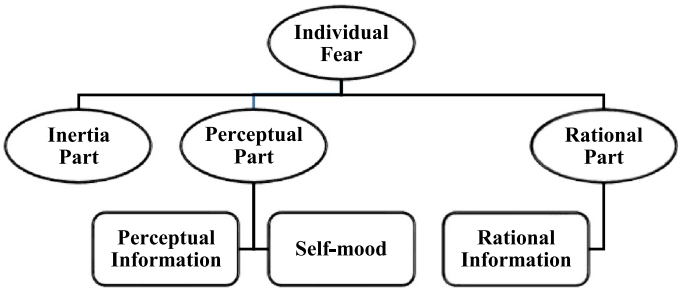

Fig. 1. Flowchart of individual fear composition.

Considering the SIR model of transmission, individuals can be divided into three states: susceptible individuals, infected individuals, and recovered individuals. The following is the classic SIR model with demography that assumes that birth rate is equal to death rate [14], then

$$\frac{dS}{dt} = -\frac{\beta SI}{N} + \alpha(N - S) \tag{2.1}$$

$$\frac{dI}{dt} = \frac{\beta SI}{N} - \gamma I - \mu I \tag{2.2}$$

$$\frac{dR}{dt} = \gamma I - \mu R \tag{2.3}$$

where S is the number of susceptible individuals, I is the number of infected individuals, R is the number of recovered individuals, β is the infection rate of individuals, γ is the recovery rate, μ is the death rate, and α is the birth rate. In here $\alpha = \mu$.

2.2. Individual fear

As stated, Geer [10] first introduced the concept of a fear factor that could quantify the human emotion of fear. Parkinson [15] reviewed emotional contagion and social appraisal and proposed that people can obtain similar emotions from their contact network via communication, meaning that fear can spread among individuals. Epstein et al. [16] incorporated fear into classic mathematical epidemiology by distinguishing behaviors of infected and recovered individuals as motivated by fear and unfear. Chen [17] investigated the relationship between information and disease transmission, such as whether an individual's fear of a disease is aggravated by information from face-to-face communication, social media, or TV broadcast, and how fear of a disease relates to the individual (e.g., individual's robustness or happiness).

In this paper we categorize IFF into perceptual, rational, and inertia parts, as shown in Fig. 1.

The perceptual part contains perceptual information and self-mood [18]. Perceptual information is affected by a local social network (i.e., face-to-face contacts such as friends, colleagues, and family members), a global social network (i.e., face-to-screen contacts such as friends in social media and people in the news), and an individual's previously fostered self-fear. Consequently, people

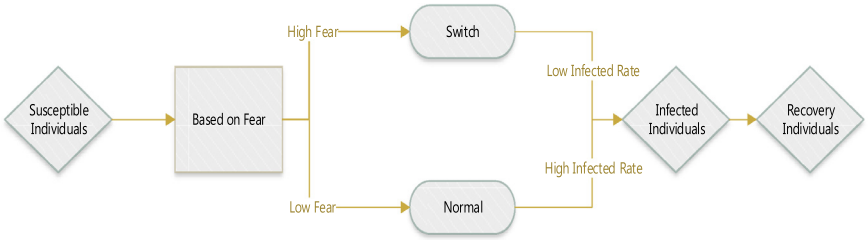

Fig. 2. Flowchart of SIR population transition and switch behavior.

in one's social network (local and global) can transfer fear into an individual. Although self-mood is a random factor, it can also affect an individual's fear factor. For example, a person may experience decreased fear toward a disease if he or she wins a large sum of money.

The rational part, however, contains rational information such as the numbers of infected and switch individuals in a local social network and a global social network. Consequently, the more people who are infected in one's social network, the more fear an individual will feel. Moreover, if an individual perceives that others are increasing use of protective measures such as masks, then that individual could also experience increased fear.

Emotions have commonly been recognized as continuous in the time series [19,20]. Suls et al. [21] first introduced the concept of emotional inertia to describe emotional fluctuation, meaning that a person's previous emotions or feelings of fear can be influenced by current emotions. Researchers have observed that emotions can be high or low in fluctuation and high or low in inertia, high in fluctuation, or low in inertia [22,23,24]. However, because researchers cannot agree on the proportion between fluctuation and inertia, we use inertia weight w in the inertia part to describe this uncertain relation, meaning that the inertia part of IFF may have different number in different situation.

2.3. Changes in human behavior

Zhao et al. [25] recently proposed a methodology that combines information dissemination, contact networks, and human behavior changes in order to model the dynamics of infectious diseases. Their study divided susceptible individuals into switch and normal individuals. Switch individuals indicated fear of the disease and potentially protected themselves by wearing masks, becoming vaccinated, or limiting their travel. Normal individuals demonstrated no change in their behavior and did not take any preventive measures to reduce their chances of infection. Although their research defined a switch behavior game for susceptible individuals, the game was based only on information and did not include mental activity.

Steimer [26] defined fear as a motivational state aroused by specific stimuli that results in defensive behavior or escape, meaning that switch behavior depends on an individual's degree of fear. Individuals with fear (or concerns) will likely take actions to protect themselves from a disease. Although research has shown that stress and fear reactions in response to infectious disease are normal and potential adaptation or protection [27], the research has not related fear to switch behavior. Therefore, in this paper, we assume that the fear factor is highly relevant to the level of switch behavior (Fig. 2), meaning that if the fear factor is high, individuals will likely choose switch behavior to protect themselves. If the fear factor is low, however, individuals will likely demonstrate normal behavior, and if the fear factor is moderate, then the potential for an individual to switch his or her behavior is more indifferent. We assume that the relationship between the fear factor and switch behavior is not constant i.e., each individual would choose to switch randomly with a probability based on the logistic probability distribution [28]. However, switch behavior is not always ideal for susceptible individuals since switching their current behaviors almost always incur certain associate costs directly or indirectly. For example, an individual may need to purchase protective measures such as face masks and vaccines, or individuals may experience loss of income or business opportunities due to reduced travel level. This paper discusses the trade-offs between protection and reduction of unnecessary cost in Section 5, and considers the reduction of possible financial loss and decreased numbers of infected individuals in the objective function.

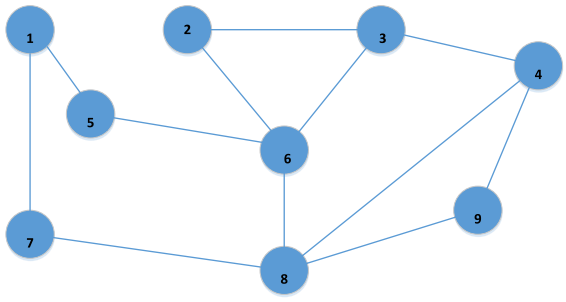

Fig. 3. Local contact networks of individuals.

2.4. Contact network

A contact network originates from a computer network, which frequently applied in the fields of electrical engineering, telecommunications, and computer science [29]. Other people in an individual's contact network can be divided into local and global contacts. Local contacts have a close relationship with the individual (e.g., family members and colleagues). Individuals 2, 3, 5, and 8 in Fig. 3 are local contacts of individual 6, and all individuals in the group are global contacts of individual 6. Meyers et al. [30] studied contact networks by inserting the concept of a contact network into a compartmental SIR model. Scoglio et al. [29] introduced a generalized epidemic modeling framework (GEMF) in order to show an individual-based network. Sahneh and Scoglio [31] researched competitive epidemic spreading on multilayer networks, these networks include both disease transmissions and information contact networks.

Local and global contacts are considered in our model. Local contacts can transfer diseases and fear to an individual, while global contacts can only transfer fear by information and emotion. Hence, the effects on disease information from local contacts frequently are more influential than that from global contacts. Since each individual cannot know exactly how many infectious and switch individuals are present in their contact network, we utilize a (random) discount between the real information and the individual received information.

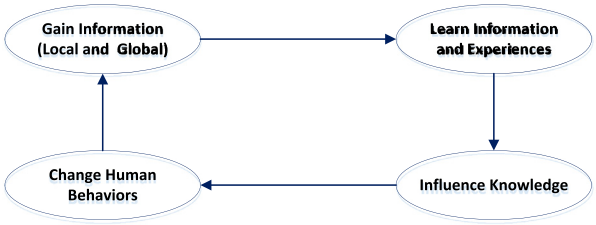

Fig. 4. Information-behavior process.

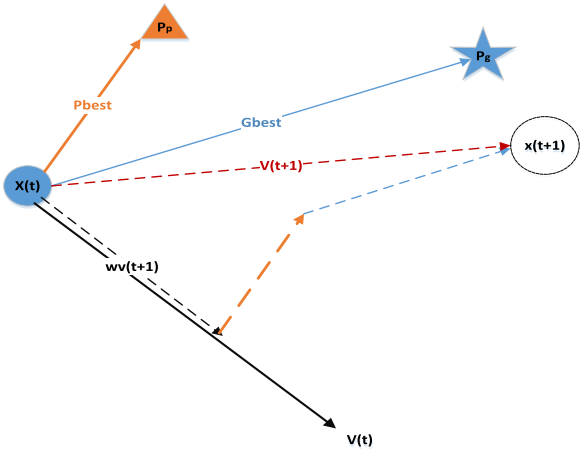

Fig. 5. Particle swarm optimization.

2.5. Particle swarm optimization (PSO)

Kennedy and coworkers [32] developed traditional PSO in an effort to produce computational intelligence by exploiting social interaction that originated from the feeding behavior of a bird flock. PSO is an evolution process from disorder to order that assumes individuals in the group as sharing information such that the entire group can determine the optimal solution. Initially, all the birds did not know where the food was, but they knew the distance between themselves and the food. Each bird shared information with other birds in the group in order to increase understanding of the food and determine more efficient behavior in order to increase their proximity to the food. Inertia caused each bird's movement to be influenced by its local known position, and all birds were guided by information in the search-space. The entire group of birds engaged in social learning (i.e., sharing information) in order to improve direction and determine the most efficient path to food.

Based on information transmission analysis, each individual in a group shares information with others. Bandura [33] stated that individual behavior can be shaped and controlled by environmental influences and internal dispositions. In the same article, the authors stated that individuals gain understanding of diseases and experiences via information derived from personal experiences and others in their group. That information is then used to determine subsequent actions. Such social learning occurs unintentionally in an individual's immediate environment. As shown in Fig. 4, individuals gain information, learn from experiences influence knowledge, and change human behavior. Human behavior is regarded as self-information that influences subsequent human behavior, similar to the feeding behavior of the bird flock.

As shown in Fig. 5, $x(t)$ represents the original position of a particle in our model (the original IFF of each individual), p_g shows the best position in the global contact networks, and p_p is the best position for the individual. Based on global and local information and in conjunction with original information, the particle would go to $x(t+1)$ along the direction of $v(t+1)$. In our model $x(t+1)$ would be the response to the next IFF and p_g, p_p would be the information an individual receives. Based on original, local, and global information, the next IFF would also tend to $x(t+1)$ along the direction of $v(t+1)$.

In PSO with inertia weight the velocity and position of particle p at iteration t are

$$v_p(t+1) = wv_p(t) + c_1 r_{1,p}(t)(p_p(t) - x_p(t)) + c_2 r_{1,p}(t)(p_g(t) - x_p(t)) \quad (2.4)$$

$$x_p(t+1) = x_p(t) + v_p(t+1) \quad (2.5)$$

where $v_p(t)$ is velocity of the pth particle ($v_p(t+1) \in [-V_{max}, +V_{max}]$), which represents decrement of IFF; $x_p(t)$ is position of the pth particle, which represents IFF in this paper; $p_p(t)$ is the best position found by the pth particle; $p_g(t)$ is the best position found by the swarm; $r_{1,p}(t)$ and $r_{2,p}(t)$ are two independent random numbers uniformly distributed on [0, 1]; c_1 is the cognitive learning factor, which represents the attraction of a particle to its own success $p_p(t)$; c_2 is the social learning factor, which represents the attraction of a particle to the swarm's best position $p_g(t)$; and w is inertia weight.

We unprecedentedly use the PSO method to describe the decrement of IFF. Since IFF could change over time, a decrement factor $dIFF/dt$ appraises the difference between previous and present fear factor. The PSO method accurately generalizes information from global and local contact networks. The PSO can be also used to describe that the IFF will change as the change of individual's emotion or opinions. We also known individual's emotion is sensitive [34], which means that his/her emotion would lead IFF tending to move to the best IFF (the best IFF will be discussed in Section 2.6).

2.6. Individual fear factor definition

This paper summarizes concepts of the PSO method, contact network, and individual fear in order to formally model and quantify the IFF. A negative IFF indicates increased confidence for an individual and a low probability that he or she would choose to switch. A positive IFF indicates less confidence for an individual and potentially higher probability of switching behavior. We suppose the maximum IFF to be 1 and the minimum IFF to be –1 and then calculate the possibility of switch base on the IFF We order the highest IFF in global contact network as 1 and the lowest IFF as −1 and assign other IFFs by linear scaling.

As stated in Section 2.2, IFF is divided into perceptual part, rational part, and inertia part, for which we use perceptual fear factor P_f, rational fear factor R_f, and inertia factor $wr_0(t)$ (w is inertia weight, t is epoch t). Perceptual fear factor P_f contains two parts, P_{fi} and P_{fm}, which represent perceptual fear from information and perceptual fear from mood, respectively. Rational fear factor R_f contains R_{fi}, which represents rational fear from information.

We use the PSO model to analyze individual behavior as

$$\frac{dIFF(t+1)}{dt} = w\frac{dIFF(t)}{dt} + P_f + R_f \quad (2.6)$$

where:

$$P_f = P_{fi} + P_{fm} \quad (2.7)$$

$$R_f = R_{fi} \quad (2.8)$$

2.6.1. Perceptual fear factor from information P_{fi}

Increasing development of transportation and communication technologies has increased the dissemination of disease information and subsequent fear of disease. People can obtain P_{fi} from local social networks as well as global social networks such as social

media. Therefore, P_{fi} contains $P_{fi-local}$ and $P_{fi-global}$, which represent P_{fi} from local contact network, global contact network, and the individual oneself. All individual moves their IFF to a position of optimal personal advantage. Undoubtedly, this position is the smallest IFF at each level when no individual is infected since an individual would switch to the smallest probability in order to minimize the cost of switch behavior. No individual is infected, so no disease spreading occurs. The information of infected individuals is rational information.

Therefore, in the perceptual part, people tend to move forward to the smallest IFF position in their local and global contact networks. Let $p_l(t)$ and $p_g(t)$ denote the smallest IFF in local and global contact networks, respectively, when no individual is infected until time t. In addition, perceptual information may contain errors between the transmitter and the receptor, so IFF may be amplified or shrunk in information transition. We assume $r_{1,p}(t)$, $r_{2,p}(t)$ to be two identical independent random numbers following Uniform distribution between [0, 1] to represent this perceptual information transition error, and we control the proportion of different information sources, where c_1 and c_2 are social learning factors of local and global social learning.

$$P_{fi} = P_{fi-local} + P_{fi-global}, \tag{2.9}$$

where

$$P_{fi-local} = c_1 r_{1,p}(t)(p_l(t) - IFF(t)) \tag{2.10}$$

$$P_{fi-global} = c_2 r_{2,p}(t)(p_g(t) - IFF(t)) \tag{2.11}$$

2.6.2. Perceptual fear factor from mood P_{fm}

Self-mood has been shown to influence fear factor [35]. For example, even though no one around an individual chooses to switch, other events such as weather, work issues could influence the mood of an individual to choose to switch. We use $m_p(t)$ which denotes a random number representing an individual's self-mood; c_3 is a self-learning factor from self-mood; and $r_{3,p}(t)$ is assumed to be an independent random variable following Uniform distribution between [0, 1].

$$P_{fm} = c_3 r_{3,p}(t) m_p(t) \tag{2.12}$$

2.6.3. Rational fear factor from information R_{fi}

Since high percentages of infected individuals and switch individuals intensifies fear within one's contact networks, the rational fear factor is based on how many infected individuals are present in a social contact network and how many individuals choose to switch in local and global contact networks. In Eqs. (2.13)–(2.15), R_{fi} contains $R_{fi-local}$ and $R_{fi-global}$, which represent R_{fi} from the local contact network, and the global contact network, respectively. $S_{l-switch}(t)$ and $S_{g-switch}(t)$ represent the numbers of switch individuals in local and global contact networks, respectively, at time t; $r_{4,p}(t)$, $r_{5,p}(t)$ are independent random numbers following Uniform distribution between [0, 1] that represent errors between real facts and rational information obtained by an individual, respectively; c_4 and c_5 are rational factors related to the number of infected individuals in a local contact network; and n_{11}, n_{12}, n_{21}, n_{22} are weights to balance the proportion of various factors.

$$R_{fi} = c_4 r_{4,p}(t) \quad R_{fi-local} + c_5 r_{5,p}(t) \quad R_{fi-global} \tag{2.13}$$

where:

$$R_{fi-local} = n_{11} I_{local}(t) + n_{12} S_{l-switch}(t) \tag{2.14}$$

$$R_{fi-global} = n_{21} I_{global}(t) + n_{22} S_{g-switch}(t) \tag{2.15}$$

2.6.4. Probability of switching

Section 2.2 described switch behavior based on IFF with a random relation that follows logistic distribution [28]. Therefore, we use function $f(IFF(t))$ to represent the probability that an individual chooses to switch under IFF. Responses are classified based on their IFF to two cases: switch and not switch. θ is the coefficient to amplify IFF since IFF is only a number at [−1,1], we assume $\theta = 100$ to make sure that $\exp(IFF(t)\theta)$ approaches to zero in our IFF model simulation. Probabilities for a normal individual to switch behaviors (e.g., taking protective measures) can be defined as follows:

$$P(do\ switch) = f(IFF(t)) = \frac{exp(IFF(t)\theta)}{1 + exp(IFF(t)\theta)} \tag{2.16}$$

$$P(do\ not\ switch) = 1 - f(IFF(t)) = \frac{1}{1 + exp(IFF(t)\theta)} \tag{2.17}$$

In Eqs. (2.16) and (2.17), if $IFF(t) \to 1$, then $P(do\ switch) \to 1$; otherwise if $IFF(t) \to -1$, then $P(do\ not\ switch) \to 1$. Each individual is evaluated a decision variable $S^p(t)$ used to record switch behaviors of individual p. $S^p(t)$ is calculated based on binomial distribution of $P(do\ switch) = f(IFF(t))$. If $S^p(t) = 1$, then an individual is expected to choose switch behavior to protect himself; if $S^p(t) = 0$, then the individual is expected to choose the behavior like normal. The total switch individuals of susceptible individuals at time t is

$$S_{switch}(t) = \sum_{p=1}^{S} S^p(t) \tag{2.18}$$

Each susceptible individual occupies $\frac{1}{S(t)}$ of susceptible individuals, their switch probability is $f(IFF(t)^p)$, and the switch probability for the average IFF of all individuals is $f(\overline{IFF(t)})$. Since the variable $\overline{IFF(t)}$ must describe IFF in an entire population as described in Section 2.7, we assume the total switch population to be equal to the average fear variable multiple susceptible population:

$$S_{switch}(t) = S(t) \sum_{p=1}^{S} \frac{f\left(IFF(t)^p\right)}{S(t)} \approx S(t) f\left(\overline{IFF(t)}\right). \tag{2.19}$$

Therefore,

$$\begin{aligned} \frac{dS_{switch}(t)}{dt} &= \frac{d\left[S(t) f\left(\overline{IFF(t)}\right)\right]}{dt} = f\left(\overline{IFF(t)}\right)\frac{dS(t)}{dt} + S(t)\frac{df\left(\overline{IFF(t)}\right)}{dt} \\ &= f\left(\overline{IFF(t)}\right)\frac{dS(t)}{dt} + \frac{S(t) d\left(\frac{\exp\left(\overline{IFF(t)}\theta\right)}{1+\exp\left(\overline{IFF(t)}\theta\right)}\right)}{dt} \\ &= f\left(\overline{IFF(t)}\right)\frac{dS(t)}{dt} + \frac{S(t)\left(\theta \exp\left(\overline{IFF(t)}\theta\right)\right)}{\left(1+\exp\left(\overline{IFF(t)}\theta\right)\right)^2}\frac{d\overline{IFF(t)}}{dt} \end{aligned} \tag{2.20}$$

2.7. The IFF-SIR model

A classic SIR model is typically used to analysis long-term epidemics. Zhao et al. [25] and Shakeri et al. [36] compiled switch behaviors into an SIR model. Sections 2.2 and 2.6 described how IFF can affect switch behaviors, but this section extends IFF to the SIR model.

$$\frac{dS(t)}{dt} = \mu N(t) - [\beta_a S_{switch}(t) + \beta_b (S(t) - S_{switch}(t))] - \mu S(t) \tag{2.21}$$

$$\frac{dI(t)}{dt} = [\beta_a S_{switch}(t) + \beta_b (S(t) - S_{switch}(t))] - \mu I(t) - \gamma I(t) \tag{2.22}$$

Table 1
Table of parameter values for numerical simulation.

Parameters	Description	Estimated values	Source
w	Inertia weight	0.729	[37]
c_1	Social learning factor toward to p_p^t	1.494	[37]
c_2	Social learning factor toward to p_g^t	1.494	[37]
c_3	Perceptual factor due to self-mood	0.001	Assume
c_4	Rational factor of local contact network	0.02	Assume
c_5	Rational factor of global contact network	0.005	Assume
θ	Coefficient number	1000	Assume
μ	Death rate (equal to birth rate)	0.019896	[38]
β_a	Infection rate of switch individuals	0.006	Assume
β_b	Infection rate of normal individuals	0.02	Assume
γ	Recovery rate	0.14	Assume

$$\frac{dR(t)}{dt} = \gamma I(t) - \mu R(t) \tag{2.23}$$

$$\frac{dS_{switch}(t)}{dt} = f\left(\overline{IFF(t)}\right)\frac{dS(t)}{dt} + \frac{S(t)\left(\theta\exp\left(\overline{IFF(t)}\theta\right)\right)}{\left(1+\exp\left(\overline{IFF(t)}\theta\right)\right)^2}\frac{d\overline{IFF(t)}}{dt} \tag{2.24}$$

$$\frac{d\overline{IFF(t)}}{dt} = \frac{dF(S(t), I(t), R(t), S_{switch}(t))}{dt} \tag{2.25}$$

In Eqs. (2.21)–(2.25), $S(t)$ denotes the number of susceptible individuals at time t; $I(t)$ is the number of infected individuals at time t; $R(t)$ denotes the number of recovered individuals at time t; $S_{switch}(t)$ is the number of susceptible individuals who adopt switch behaviors at time t; $N(t)$ is the total number of individuals at time t, of which $N(t) = S(t) + I(t) + R(t)$; β_a and $\beta_b$are infection rates of susceptible individuals who choose switch or normal behavior, respectively; γ is the recovery rate; and μ is the death rate. (The birth rate is assumed to be equal to the death rate.)

We consider IFF to be the primary factor for an individual who decides to switch or not, but we are unable to add all IFF of each individual as variables into our dynamic system for simplify the calculation efforts when deal with the total population is large. Since we already defined $\overline{IFF(t)}$ as the average of all IFF in switch individuals at time t, we can calculate $\overline{IFF(t)}$ for any time $t = 0, 1, 2, 3, \ldots\ldots, n$. However, because we do not know the mathematical relationship between $\overline{IFF(t)}$ and $S(t)$, $I(t)$,$R(t)$, $S_{switch}(t)$, we will use simulation to establish these relationships in Section 3.1 and conduct linear regression to obtain the mathematic relationship function.

3. Simulation and regression analysis

3.1. Numerical simulation

This section details a MATLAB simulation of epidemic transmission and the corresponding fear factor. The simulation runs span 50 days, each time epoch is 1 day [8]. We also assume that the total number of individuals in global contact network is $N = 200$: 185 susceptible individuals, 15 infected individuals, 0 recovered, and 0 switched susceptible individuals. To simplify the simulation, we assume the status changing probability from infected to recovered is 14% at each day. The values of other parameters are given in Table 1.

Fig. 6 illustrates the change in the number of individuals in each state. The red solid line represents recovered individuals, the green dash-dot line represents infected individuals, the blue dashed line represents susceptible individuals, and the black dotted line represents switched susceptible individuals. As shown in the figure, the disease was active almost 20 days, with the highest number of infections occurring around day 7. Susceptible, infected, and recovered individuals stay the same after day 20, with only rare occurrences of individuals choosing switch behavior after 20 days.

Table 2
Variance of average IFF regression analysis.

Source	Degree of freedom	Coef	F-value	T-value	P-value
I	1	−0.00008	0.00	−0.02	0.983
S	1	−0.01172	28.91	−5.39	0.000
S_{switch}	1	0.09768	139.11	11.79	0.000
I^*S	1	0.000363	9.36	3.06	0.004
I^* S_{switch}	1	−0.002846	46.75	−6.84	0.000
Lack-of-fit	4		0.84		0.508

Fig. 7 shows the average IFF for all susceptible individuals over the first 50 days in a disease. In SIR model, all individuals just can be infected one time, after recovery they will never be infected, thus considering the IFF of recovered individuals and infected individuals is meaningless for our model. Therefore, we just consider switch individuals from susceptible individuals. In addition, since the delay of time, switch behaviors this time will have influence on IFF in next time rather than immediately influence their IFF this time, which is demonstrated by the trend of infected and switch individuals shown in Fig. 6. This phenomenon explains how the past information persistently effects the current emotion when people face to a disease. After the increasing number of infectious and switch individuals on day 3 and day 4, the average IFF suddenly increased on day 5. After day 15, as infected and switch individuals tend to stable, the IFF also tend to stable.

3.2. Regression analysis

In order to establish a precise relationship between $\overline{IFF(t)}$ and population sizes in each state, we make multiple-variate linear regressions of $\overline{IFF(t)}$ and susceptible individuals using the statistical analysis tool Minitab. For model simplicity, we only considered nonlinear cross-term in regression but did not use the nonlinear regression.

We use $\overline{IFF(t)}$ as the dependent (response) variable y and $S(t)$, $I(t)$, $R(t)$, $S_{switch}(t)$ as independent variables. The data of regression was based on the average variable numbers (by 10 replications) with initial $N = 200$; $S = 185$; $I = 15$; $R = 0$; $S_{switch} = 0$. Then we find the regression relationship using the optimized response regression toolbox in Minitab. We reject the last section $r_5 I(t)$ due to the high P-value and low F-value and T-value, as shown in Table 2. The correlation coefficients between $I(t)$ with $S(t)I(t)$ and $S_{switch}(t)I(t)$ are 0.924 and 0.925, respectively, proving that $I(t)$ is not significant in this model. Although $I(t)$ becomes significant when we try to make linear regression without cross-terms, the

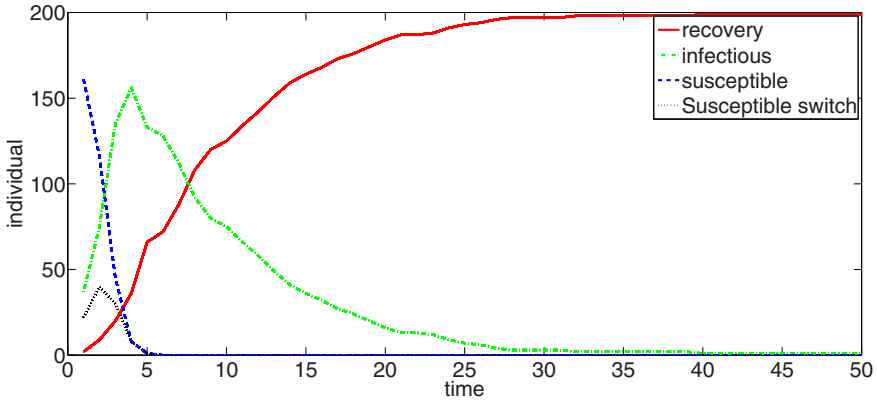

Fig. 6. Populations in each state during the epidemic. (For interpretation of the references to color in this figure, the reader is referred to the web version of this article).

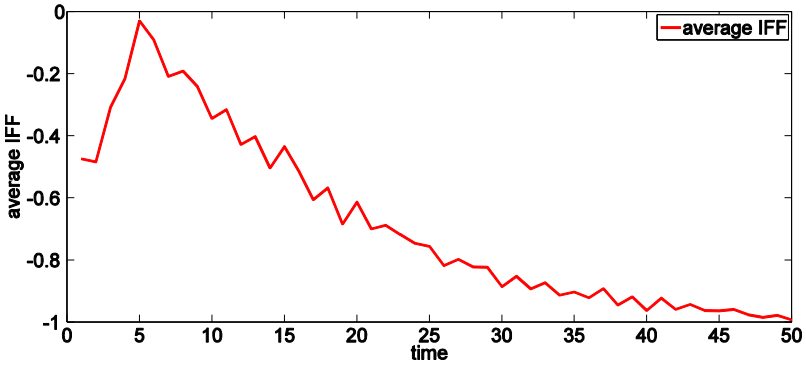

Fig. 7. Average IFF of susceptible individuals during the epidemic.

R-square of the new regression model decreases significantly.

$$\overline{IFF(t)} = r_0 + r_1 S(t) + r_2 S_{switch}(t) + r_3 S(t) I(t) - r_4 S_{switch}(t) I(t) + r_5 I(t) \tag{3.1}$$

where $r_0 = -0.5902$, $r_1 = -0.01172$, $r_2 = 0.09768$, $r_3 = 0.000363$, $r_4 = 0.002846$, and $r_5 = -0.00008$.

The P-value result to be less than 0.001 [39], proving that the regression model is statistically significant. Because we used the optimized response regression, all five sections (including constant term r_0) in our regression model are significant. Fig. 8 also shows the R-square number of the model to be 92.59%, meaning that 92.59% of the variation in $\overline{IFF(t)}$ can be explained by the regression model. The optimized response indicates a potentially higher R-square with the use of more sections, but the effect is not sufficiently significant. In addition, the absolute value of a majority of residuals is less than 0.02, meaning that most $\overline{IFF(t)}$ can be accurately represented by the regression model in Eq. (3.1). The highest absolute value of residual is approximately 0.05, proving general reliability of the regression model.

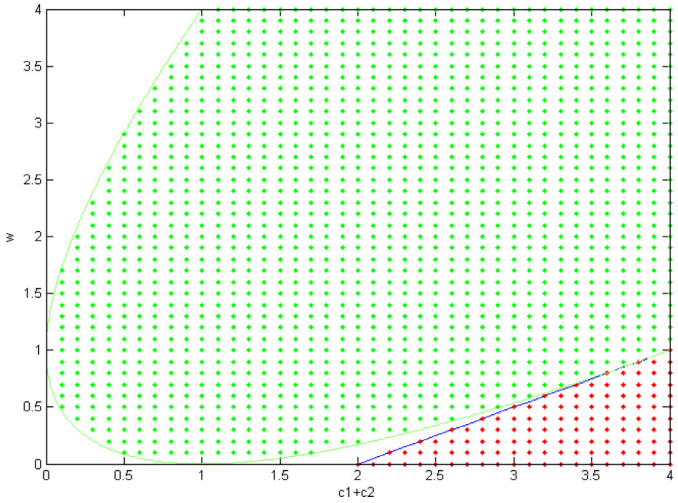

Fig. 8. Convergence area (green area) and non-convergence area (red area) of IFF(t). (For interpretation of the references to color in this figure legend, the reader is referred to the web version of this article).

4. Stability analysis

4.1. Stability analysis of the IFF model

In order to conduct stability analysis of the IFF model and determine necessary conditions we first need to define the stable status. Two kinds of stability are typical: absolute stability and asymptotic stability. Because several random numbers in our system represent self-mood and the random weight of various information, determining a clear definition of the convergence domain of asymptotically stable status is difficult. Therefore, in this section we discuss only absolute stability.

Definition 1. [40]: For a continuous nonlinear system, $\dot{x} = f(x(t))$, $x(0) = x_0$, where $x(t) \in S \subseteq \mathbb{R}^n$ are system-state variables, S is an open set on $\mathbb{R}^n$, and f is a continuous function on S. The system is Lyapunov stable in equilibrium state x_e if for every $\epsilon > 0$ there is $\delta > 0$ such that

$$\|x(0) - x_e\| < \delta \tag{4.1}$$

Then for every $t \geq 0$,

$$\|x(t) - x_e\| < \epsilon \tag{4.2}$$

Theorem 1. *If the IFF model is stable, then* $IFF(t) = -1$ *and* $R_{fi} = 0$.

Proof. To prove contradiction, first we assume that $IFF(t)$ is not constant, and assume there are two different IFF values presenting in the system with a total of N individuals. Then n individuals have $IFF(t) = IFF(1)$ and $N-n$ individuals $IFF(t) = IFF(2)$.

Let $IFF(1) > IFF(2)$. Then based on the meaning of P_{fi}, $IFF(1)$ will move toward $IFF(2)$, while some individuals with fear factors of $IFF(1)$ will switch because $IFF(1) > IFF(2) \geq -1$, and then $S_{switch} > 0$ and $R_{fi} > 0$. In this situation, $N-n$ individuals will increase, meaning the IFF model is unstable. If $IFF(1) < IFF(2)$, then the situation is equal to $IFF(1) > IFF(2)$, resulting in a contradiction unless $IFF(1) = IFF(2)$, which means that $IFF(t)$ does not change over time when the IFF model is stable. Therefore, $IFF(t) = C$ (C is a constant) and $R_{fi} = 0$ are requirements of system stability for all individuals in the system, and stable status should occur in a disease-free situation ($S_{switch} = 0,\ I = 0$).

We already proved that individuals must have identical IFF in order for the IFF model to be stable, but in order to prove contradiction of $IFF(t) = -1$, now we assume that the IFF is a constant larger than -1. Since switch behaviors of individuals are based on IFF, we assume that individual would choose to switch randomly.

If individual chooses to switch as event A, the probability of event A is $P(A) = \varepsilon > 0$ (since $\varepsilon = 0$ only happened in $IFF(t) = -1$ as mentioned in Section 2.6), where ε is a positive number. Therefore, the probability for individual not choosing to switch is $1-\varepsilon$. No matter how small ε is, when the time period is long enough, the probability for individual never choosing to switch is

$$(1-\boldsymbol{\varepsilon})^{\boldsymbol{t}} \underset{\boldsymbol{t}\to\infty}{\to} 0 \tag{4.3}$$

So this individual would choose to switch at least one time in the timeline, then $S_{switch} \neq 0$, which leads to a contradiction unless the IFF of all individuals are -1, resulting in $IFF(t) = C = -1$.

Theorem 2. *If the IFF model is stable, then* $w > \frac{1}{2}(c_1 + c_2) - 1$.

Proof. If the IFF model is stable, then $IFF(t)$ will be convergent, assuming

$$\lim_{t\to+\infty} IFF(t) = p \tag{4.4}$$

where p is an arbitrary range of the value of $IFF(t)$.

Each individual in the SIR model can be infected only once. Since susceptible individuals were never infected, we consider the fear factor of susceptible individuals to be $R_{fr} = 0$. Therefore, according to Theorems 1–3, when the IFF model is stable, then

$$\frac{dIFF(t+1)}{dt} = w\frac{dIFF(t)}{dt} + c_1 r_{1,p}(t)(p_I(t) - IFF(t)) + c_1 r_{2,p}(t)(p_g(t) - IFF(t)) \tag{4.5}$$

$$IFF(t+1) = IFF(t) + \frac{dIFF(t+1)}{dt} \tag{4.6}$$

Let $\emptyset_1 = c_1 r_{1,p}(t)$ and $\emptyset_2 = c_2 r_{2,p}(t)$ [41], where $\emptyset_1$, $\emptyset_2$, and w are constant. If $\frac{dIFF(t)}{dt} = IFF(t) - IFF(t-1)$ and Eq. (4.6) is replaced by Eq. (4.5), then

$$IFF(t+1) = (1 + w - \emptyset_1 - \emptyset_2)IFF(t) - wIFF(t-1) + \emptyset_1 p_I(t) + \emptyset_2 p_g(t) \tag{4.7}$$

This non-homogeneous recurrence relation can be written as a matrix-vector equation:

$$\begin{bmatrix} IFF(t+1) \\ IFF(t) \\ 1 \end{bmatrix} = \begin{bmatrix} 1+w-\emptyset_1-\emptyset_2 & -w & \emptyset_1 p_I(t) + \emptyset_2 p_g(t) \\ 1 & 0 & 0 \\ 0 & 0 & 1 \end{bmatrix} \times \begin{bmatrix} IFF(t) \\ IFF(t-1) \\ 1 \end{bmatrix} \tag{4.8}$$

The characteristic polynomial of this matrix is

$$\left| \begin{bmatrix} IFF(t+1) \\ IFF(t) \\ 1 \end{bmatrix} - \lambda E \right| = (1-\lambda)\left(w + \lambda^2 - \lambda(1 + w - \emptyset_1 - \emptyset_2)\right) \tag{4.9}$$

which has three roots:

$$\lambda_1 = 1 \tag{4.10}$$

$$\lambda_2 = \frac{1 + w - \emptyset_1 - \emptyset_2 + \vartheta}{2} \tag{4.11}$$

$$\lambda_3 = \frac{1 + w - \emptyset_1 - \emptyset_2 - \vartheta}{2} \tag{4.12}$$

where

$$\vartheta = \sqrt{(1 + w - \emptyset_1 - \emptyset_2)^2 - 4w} \tag{4.13}$$

According to the recurrence relation, the explicit form of Eq. (4.9) is

$$IFF(t) = k_1{\lambda_1}^t + k_2{\lambda_2}^t + k_3{\lambda_3}^t = k_1 + k_2{\lambda_2}^t + k_3{\lambda_3}^t \tag{4.14}$$

where k_1, k_2, k_3 are constant.

Eq. (4.8) also produces

$$IFF(2) = (1 + w - \emptyset_1 - \emptyset_2)IFF(1) - wIFF(0) + \emptyset_1 p_I(t) + \emptyset_2 p_g(t) \tag{4.15}$$

and Eq. (4.14) yields

$$\begin{bmatrix} IFF(0) \\ IFF(1) \\ IFF(2) \end{bmatrix} = \begin{bmatrix} 1 & 1 & 1 \\ 1 & \lambda_2 & \lambda_3 \\ 1 & {\lambda_2}^2 & {\lambda_3}^2 \end{bmatrix} \begin{bmatrix} k_1 \\ k_2 \\ k_3 \end{bmatrix} \tag{4.16}$$

From Eq. (4.16) we can calculate that

$$k_1 = \frac{\lambda_2\lambda_3 IFF(0) - IFF(1)(\lambda_2 + \lambda_3) + IFF(2)}{(\lambda_2 - 1)(\lambda_3 - 1)} \tag{4.17}$$

$$k_2 = \frac{\lambda_3(IFF(0) - IFF(1)) - IFF(1) + IFF(2)}{(\lambda_2 - 1)(\lambda_2 - \lambda_3)} \tag{4.18}$$

$$k_3 = \frac{\lambda_2(IFF(1) - IFF(0)) + IFF(1) - IFF(2)}{(\lambda_3 - 1)(\lambda_2 - \lambda_3)} \tag{4.19}$$

Using the property $\lambda_2 - \lambda_3 = \vartheta$, these values can be simplified as

$$k_1 = \frac{\emptyset_1 p_I(t) + \emptyset_2 p_g(t)}{\emptyset_1 + \emptyset_2} \tag{4.20}$$

$$k_2 = \frac{\lambda_3(IFF(0) - IFF(1)) - IFF(1) + IFF(2)}{(\lambda_2 - 1)(\lambda_2 - \lambda_3)} \tag{4.21}$$

$$k_3 = \frac{\lambda_2(IFF(1) - IFF(0)) + IFF(1) - IFF(2)}{(\lambda_3 - 1)(\lambda_2 - \lambda_3)} \tag{4.22}$$

In order to identify the condition at which the IFF model is stable, we consider the relationship of w and c_1, c_2 since $\emptyset_1$ and $\emptyset_2$ are specific expressions of $c_1 r_{1,p}(t)$, $c_2 r_{2,p}(t)$, respectively. We can then determine the upper bound associated with these values using the largest value of $\emptyset_1$ and $\emptyset_2$, and the values of $c_1$and c_2 can be considered upper bounds for $\emptyset_1$ and $\emptyset_2$. Therefore, we can consider the worst-case in terms of convergence.

Convergence of $\lim_{t\to+\infty} IFF(t)$ is determined by the values of $\emptyset_1$ and $\emptyset_2$. Eq. (4.6) shows that ϑ will be a complex number with a non-zero component when

$$(1 + w - \emptyset_1 - \emptyset_2)^2 < 4w \tag{4.23}$$

or

$$(\emptyset_1 + \emptyset_2 - w - 1 - 2\sqrt{w})(\emptyset_1 + \emptyset_2 - w - 1 + 2\sqrt{w}) < 0 \tag{4.24}$$

Since ϑ is complex, λ_2 and λ_3 will be complex numbers with non-zero components.

Using the L_2 norm to measure λ_2 and λ_3, any complex number x, x^t can be

$$x^t = \left(\|x\|e^{-i\theta}\right)^t = \|x\|^t e^{-i\theta t} = \|x\|^t(\cos(\theta t) + i\sin(\theta t)) \quad (\theta = \arg(x)) \tag{4.25}$$

$$\lim_{t\to+\infty} x^t = \lim_{t\to+\infty} \|x\|^t(\cos(\theta t) + i\sin(\theta t)) = 0 \text{ if and only if } \|x\| < 1 \tag{4.26}$$

Considering the value of $\lim_{t\to+\infty} IFF(t)$, thus

$$\lim_{t\to+\infty} IFF(t) = \lim_{t\to+\infty} k_1 + k_2{\lambda_2}^t + k_3{\lambda_3}^t \tag{4.27}$$

When $\|\boldsymbol{\lambda}_2\| < 1$ and $\|\boldsymbol{\lambda}_3\| < 1$, then $\lim_{t\to+\infty} {\lambda_2}^t = 0$ and $\lim_{t\to+\infty} {\lambda_3}^t = 0$.

Assuming uniform distributions, $\emptyset_1 \sim U(0,1)$ and $\emptyset_2 \sim U(0,1)$, then

$$E[\emptyset_1] = c_1 \int_0^1 \emptyset_1 d\emptyset_1 = \frac{c_1}{2} \tag{4.28}$$

$$E[\emptyset_2] = c_2 \int_0^1 \emptyset_2 d\emptyset_2 = \frac{c_2}{2} \tag{4.29}$$

Thus,

$$\lim_{t\to+\infty} IFF(t) = k_1 = \frac{\emptyset_1 p_l(t) + \emptyset_2 p_g(t)}{\emptyset_1 + \emptyset_2} = \frac{\frac{c_1}{2} p_l(t) + \frac{c_2}{2} p_g(t)}{\frac{c_1}{2} + \frac{c_2}{2}} = \frac{c_1 p_l(t) + c_2 p_g(t)}{c_1 + c_2} = (1-a)p_l(t) + a p_g(t) \left(a = \frac{c_2}{c_1 + c_2}\right) \tag{4.30}$$

proving that $IFF(t)$ converges to a value from the lines $p_l(t)$ and $p_g(t)$.

As shown in Fig. 8, $\emptyset_1 + \emptyset_2$ represents the horizontal axis (associated with $c_1 + c_2$), w represents the vertical axis, the green area represents the region for $(1 + w - \emptyset_1 - \emptyset_2)^2 < 4w$, and the red area represents the nonconvergent region of $IFF(t)$, resulting in $\max(\|\boldsymbol{\lambda}_2\|, \|\boldsymbol{\lambda}_3\|) > 1$ [41]. In addition, $w < \frac{1}{2}(\emptyset_1 + \emptyset_2) - 1$ (blue line is $w = \frac{1}{2}(\emptyset_1 + \emptyset_2) - 1$) in the red area. As stated, we consider the upper limits of $\emptyset_1$ and $\emptyset_2$ to satisfy $\emptyset_1 \in [0, c_1]$ and $\emptyset_2 \in [0, c_2]$ in order to determine the condition. The area to the left of the blue line ensures convergence; therefore, if we want to ensure convergence, all values of w must be larger than the values of the blue line. If the IFF model is stable, $IFF(t)$ will converge and satisfy

$$w > \frac{1}{2}(\emptyset_1 + \emptyset_2) - 1 \tag{4.31}$$

Satisfaction of these four theorems ensures that the IFF model is stable.

4.2. Stability analysis of the IFF-SIR model

In order to conduct stability analysis of the IFF-SIR model, we initially combine the regression result from Section 2.7 into the IFF-SIR model:

$$\overline{IFF(t)} = r_0 + r_1 S(t) + r_2 S_{switch}(t) + r_3 S(t) I(t) - r_4 S_{switch}(t) I(t) \tag{4.32}$$

Then

$$\frac{d\overline{IFF(t)}}{dt} = r_1\frac{dS(t)}{dt} + r_2\frac{dS_{switch}(t)}{dt} + r_3 I(t)\frac{dS(t)}{dt} + r_3 S(t)\frac{dI(t)}{dt} - r_4 I(t)\frac{dS_{switch}(t)}{dt} - r_4 S_{switch}(t)\frac{dI(t)}{dt} \tag{4.33}$$

Therefore, the model can be written as the linear system (4.34)–(4.38) and stability points of this system can be determined using

$$\frac{dS(t)}{dt} = \mu N(t) - [\beta_a S_{switch}(t) + \beta_b(S(t) - S_{switch}(t))] - \mu S(t) \tag{4.34}$$

$$\frac{dI(t)}{dt} = [\beta_a S_{switch}(t) + \beta_b(S(t) - S_{switch}(t))] - \mu I(t) - \gamma I(t) \tag{4.35}$$

$$\frac{dR(t)}{dt} = \gamma I(t) - \mu R(t) \tag{4.36}$$

$$\frac{dS_{switch}(t)}{dt} = f\left(\overline{IFF(t)}\right)\frac{dS(t)}{dt} + \frac{S(t)\left(\exp\left(\overline{IFF(t)}\right)\right)}{\left(1 + \exp\left(\overline{IFF(t)}\right)\right)^2}\frac{d\overline{IFF(t)}}{dt} \tag{4.37}$$

$$\frac{d\overline{IFF(t)}}{dt} = r_1\frac{dS(t)}{dt} + r_2\frac{dS_{switch}(t)}{dt} + r_3 I(t)\frac{dS(t)}{dt} + r_3 S(t)\frac{dI(t)}{dt} - r_4 I(t)\frac{dS_{switch}(t)}{dt} - r_4 S_{switch}(t)\frac{dI(t)}{dt} \tag{4.38}$$

Theorem 3. *The continuous-time system (4.34)–(4.38) is Lyapunov stable if the following system in Eq. (4.39) has a real solution:*

$$\begin{aligned} &N(t) - [\beta_a S_{switch}(t) + \beta_b(S(t) - S_{switch}(t))] - \mu S(t) = 0 \\ &[\beta_a S_{switch}(t) + \beta_b(S(t) - S_{switch}(t))] - \mu I(t) - \gamma I(t) = 0 \\ &\gamma I(t) - \mu R(t) = 0 \end{aligned} \tag{4.39}$$

Proof. Based on Definition 1, t^* can satisfy following condition:

$$\left[\frac{dS(t^*)}{dt^*}, \frac{dI(t^*)}{dt^*}, \frac{dR(t^*)}{dt^*}, \frac{dS_{switch}(t^*)}{dt^*}, \frac{d\overline{IFF(t^*)}}{dt^*}\right] = 0 \tag{4.40}$$

Therefore, every $t \geq 0$ will produce

$$x(t) = x(t^*) = \left[S(t^*), I(t^*), R(t^*), S_{switch}(t^*), \overline{IFF(t^*)}\right] \tag{4.41}$$

and every $\epsilon > 0$ and $t \geq t^*$ will yield to the limitation $\|x(t) - x(t^*)\| < \epsilon$.

If we find a set $x(t^*)$ resulting in $\frac{d\overline{IFF(t^*)}}{dt} = 0$ and if t^* satisfies $\frac{d\overline{IFF(t^*)}}{dt^*} = 0$, then we can find a t^* that satisfies

$$\frac{dS_{switch}(t^*)}{dt^*} = f\left(\overline{IFF(t^*)}\right)\frac{dS(t^*)}{dt^*} + \frac{S(t^*)\left(\exp\left(\overline{IFF(t^*)}\right)\right)}{\left(1 + \exp\left(\overline{IFF(t^*)}\right)\right)^2}\frac{d\overline{IFF(t^*)}}{dt^*} = f\left(\overline{IFF(t^*)}\right)\frac{dS(t^*)}{dt^*} \tag{4.42}$$

Also, because $\frac{dS(t^*)}{dt^*} = 0$, the value of $f(\overline{IFF(t^*)})$ will produce

$$\frac{dS_{switch}(t^*)}{dt^*} = f\left(\overline{IFF(t^*)}\right)\frac{dS(t^*)}{dt^*} = 0 \tag{4.43}$$

meaning that $\frac{dS_{switch}(t^*)}{dt^*}$ can be designated using $\frac{dS(t^*)}{dt^*}$ and $\frac{d\overline{IFF(t^*)}}{dt^*}$.

Therefore, the system becomes

$$\mu N(t^*) - [\beta_a S_{switch}(t^*) + \beta_b (S(t^*) - S_{switch}(t^*))] - \mu S(t^*) = 0 \tag{4.44}$$

$$[\beta_a S_{switch}(t^*) + \beta_b (S(t^*) - S_{switch}(t^*))] - \mu I(t^*) - \gamma I(t^*) = 0 \tag{4.45}$$

$$\gamma I(t^*) - \mu R(t^*) = 0 \tag{4.46}$$

$$r_1 \frac{dS(t^*)}{dt^*} + r_2 \frac{dS_{switch}(t^*)}{dt^*} + r_3 I(t^*) \frac{dS(t^*)}{dt^*} + r_3 S(t^*) \frac{dI(t^*)}{dt^*} - r_4 I(t^*) \frac{dS_{switch}(t^*)}{dt^*} - r_4 S_{switch}(t^*) \frac{dI(t^*)}{dt^*} = 0 \tag{4.47}$$

Moreover, $\frac{d\overline{IFF(t^*)}}{dt^*}$ can be indicated by $\frac{dS(t^*)}{dt^*}$, $\frac{dI(t^*)}{dt^*}$, $\frac{dS_{switch}(t^*)}{dt^*}$. Thus, the system (4.34)–(4.38) can rewrite as the system $\boldsymbol{C}$ below

$$C\begin{cases} \frac{dS(t)}{dt} = \mu N(t) - [\beta_a S_{switch}(t) + \beta_b (S(t) - S_{switch}(t))] - \mu S(t) = 0 \\ \frac{dI(t)}{dt} = [\beta_a S_{switch}(t) + \beta_b (S(t) - S_{switch}(t))] - \mu I(t) - \gamma I(t) = 0 \\ \frac{dR(t)}{dt} = \gamma I(t) - \mu R(t) = 0 \end{cases} \tag{4.48}$$

From system C, the equation set can be written as

$$\begin{bmatrix} -\beta_b & \mu & \mu & -\beta_a + \beta_b \\ \beta_b & -\mu - \gamma & 0 & \beta_a - \beta_b \\ 0 & \gamma & -\mu & 0 \\ 0 & 0 & 0 & 0 \end{bmatrix} \begin{bmatrix} S(t) \\ I(t) \\ R(t) \\ S_{switch}(t) \end{bmatrix} = c \begin{bmatrix} S(t) \\ I(t) \\ R(t) \\ S_{switch}(t) \end{bmatrix} = 0 \tag{4.49}$$

Since

$$det|c| = 0 \tag{4.50}$$

system c has infinite solutions, meaning that system (4.34)–(4.38) will be stable if the SIR model is stable, also the system has infinite stability points.

In order to verify accuracy of our result, we use the regression results to check the model. We assume the total number of individuals in the global contact network is $N = 1050$, 1000 susceptible individuals, 50 infected individuals, 0 recovered, and 50 switch individuals. We observe the trend of populations in each state and the estimated $\overline{IFF(t)}$ based on the regression model in Eq. (3.1) over 100 days, as shown in Fig. 9.

According to Fig. 9, the simulation results show that the epidemic situation become stable after approximately 70 days, the number of susceptible, infectious, recovered and switch don notchange significantly anymore after 70 days. According to the Theorem 3 we prove above and the regression result in Eq. (4.32), we can know that when SIR is stable, the IFF model should be stable. Fig. 10 shows the trend of $\overline{IFF(t)}$, it illustrates that $\overline{IFF(t)}$ is stable when the SIR model is stable (Fig. 10).

In previous regression we had restricted the range of $\overline{IFF(t)}$ to [−1, 1] and used only 200 individuals for simulation. We verify our present model using 1050 individuals, so the trend of $\overline{IFF(t)}$ would exceed the range of [−1, 1] in the real world. However, our conclusion is proven accurate: an increasing $\overline{IFF(t)}$ leads to an increasing number of individuals who will switch. Sudden increase in $\overline{IFF(t)}$ around day 2 in Fig. 9 and day 3 in Fig. 10 show a breakout of infected and switch individuals, thereby increasing individuals' fear of the disease and resulting in a sudden increase of $\overline{IFF(t)}$.

5. Optimal control

5.1. Definition for control of switch degree

We define the switch degree as ranging from 0 to 100. Therefore, if individuals chose to switch but do not undertake any measures of switching, we assume their degrees of switching, or switch behavior, to be zero.

In order to simulate the relationship between infection rates and switching behavior, we make the following three assumptions:

- The corporate social performance of each individual can be controlled.
- Infection rate is proportional to the number of contacts, and the number of contact is proportional to the corporate social performance.
- Switching behavior is determined by the corporate social performance degrees.

We add a control variable u, to represent the decreasing degrees of corporate social performance of an individual; therefore, $(1 - u)$ represents the corporate social performance. According to above assumptions, u represents the degrees of switching. If an individual decreases degrees of corporate social performance, thereby decreasing the number of contacts, that individual decreases his or her chances of being infected with the disease. More reductions of corporate social performance degrees result in decreased degrees of corporate social performance and increased degrees of switching.

If $u = 0$, then individuals do not have any degree of switching, but they choose to switch. Since their corporate social performance has not decreased, the number of contacts is the same as the individuals who did not switch. Consequently, the infection rate does not change and stays equal to normal behavior, or β_b.

According to the second assumption,

$$\frac{\beta_a}{\beta_b} = \frac{1 - u}{1}, \quad u \in [0,\ 1] \tag{5.1}$$

Although all individual p should have a best control u_p, the IFF set in our model may be too large and impractical to control the corporate social performance for all individual, requiring control of the average of all corporate social performances as u instead. For example, if the best controls of three individuals are assumed to be 0.3, 0.5, and 0.7, respectively, those values can be controlled by average $u = \frac{0.3+0.5+0.7}{3} = 0.5$.

Finally,

$$\beta_a = \beta_b (1 - u), \quad u \in [0,\ 1] \tag{5.2}$$

5.2. Optimal control problem

The first part of the cost function $F(I)$ is the number of infected individuals, and the second part of the cost function $F(S_{switch})$ is associated with financial loss of switch behaviors. Switch behaviors in our model indicate that an individual chooses to decrease his or her corporate social performance. Therefore, the cost function is

$$J(u) = \int [F(I(t)) + F(S_{switch}(t))] dt \tag{5.3}$$

Loss function $F(I)$ relates to all infected individual, resulting in cost payoffs during the process of disease infection, such as income and revenue loss for the infected individual and associated medical costs. If all infected individual is assigned a fixed cost z, then the cost of all infected individuals can be expressed as

$$F(I(t)) = zI(t) \tag{5.4}$$

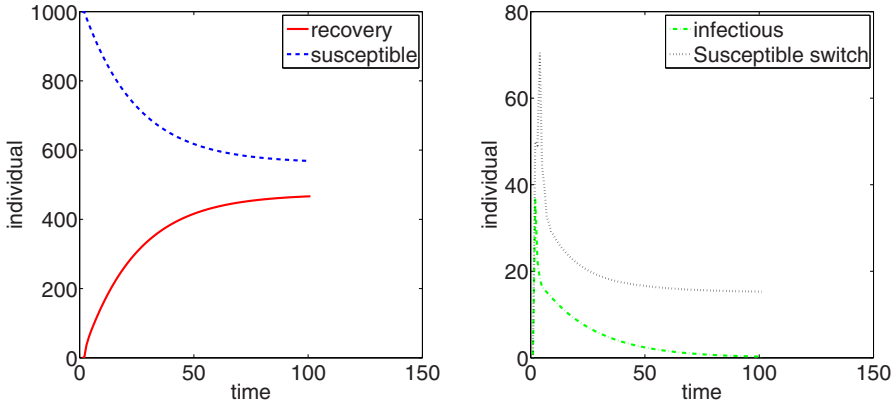

Fig. 9. Populations in each state during the epidemic by IFF-SIR model.

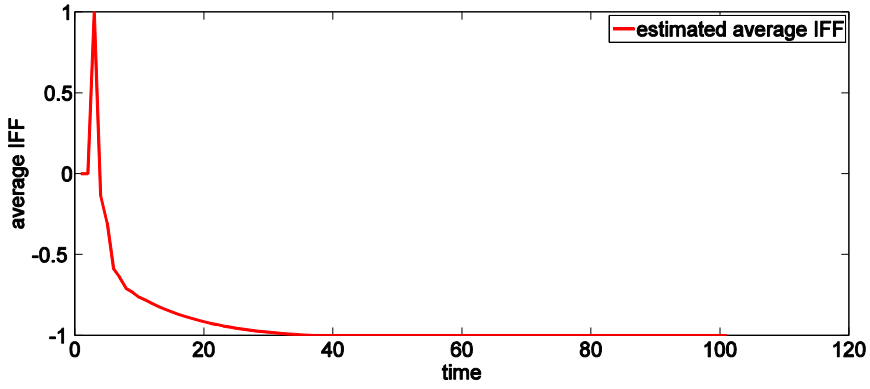

Fig. 10. Estimated result of average IFF(t) by IFF-SIR model.

Evidence suggests that a higher degree of corporate social performance could improve financial benefits for that performance. Research [42] suggests that expected improvements in social performance could lead to improvements in financial performance, thereby decreasing financial loss. However, excessively large degrees of corporate social performance could have a negative financial impact. For example, an individual's large degree of corporate social performance could reduce payoffs from social networks [43].

Brammer et al. [43] studied the relationship between corporate social performance and corporate financial performance and determined that corporate financial performance, which is a quadratic function of the corporate social performance, provides no financial payoffs to normal corporate social performance. In our model, $(1-u)$ represents corporate social performance, u represents corporate social performance reduction, and $F(S_{switch}(t))$ represents financial loss and payoffs due to the corporate social performance. According to [43] and our description, a relationship between corporate social performance and financial loss can be assumed to be a positive quadratic relation. When $u>0$, an increasing corporate social performance degree $(1-u)$ means a decreasing number of individuals would choose to switch, leading to decreased financial loss. When no one switches and all individuals maintain normal corporate social performance, no financial loss results (i.e., when $u=0$, then $1-u=1$ and financial loss is zero). However, when the corporate social performance degree reaches a specific point (e.g., $u<0$), it generates a negative financial impact. Therefore, the larger the corporate social performance degree $(1-u)$, the greater the financial loss.

The relationship between financial loss and corporate social performance can be expressed by

$$F(S_{switch}(t)) = b_1(1-u-b_2)^2 S_{switch}(t) \tag{5.5}$$

where z represents the average financial loss associated with each infected individual and b_1 and b_2 represent the scaling and shift parameters, respectively. Constraint conditions of the optimal control problems are

$$g_1 = \frac{dS(t)}{dt} - \mu N(t) - [\beta_b(1-u)S_{switch}(t) + \beta_b(S(t) - S_{switch}(t))] - \mu S(t) \tag{5.6}$$

$$g_2 = \frac{dI(t)}{dt} = [\beta_b(1-u)S_{switch}(t) + \beta_b(S(t) - S_{switch}(t))] - \mu I(t) - \gamma I(t) \tag{5.7}$$

$$g_3 = \frac{dR(t)}{dt} = \gamma I(t) - \mu R(t) \tag{5.8}$$

$$g_4 = \frac{dS_{switch}(t)}{dt} = f\left(\overline{IFF(t)}\right)\frac{dS(t)}{dt} + \frac{S(t)\exp\left(\overline{IFF(t)}\right)}{\left(1+\exp\left(\overline{IFF(t)}\right)\right)^2}\frac{d\overline{IFF(t)}}{dt} \tag{5.9}$$

$$g_5 = \frac{d\overline{IFF(t)}}{dt} = r_1\frac{dS(t)}{dt} + r_2\frac{dS_{switch}(t)}{dt} + r_3 I(t)\frac{dS(t)}{dt} + r_3 S(t)\frac{dI(t)}{dt} - r_4 I(t)\frac{dS_{switch}(t)}{dt} - r_4 S_{switch}(t)\frac{dI(t)}{dt} \tag{5.10}$$

5.3. Necessary optimality condition

Using Pontryagins maximum principle [44], the optimal control problem can be reduced to minimize Hamiltonian function H:

$$H(u,\ S,\ I,\ R) = F(I(t)) + F(S_{switch}(t)) + \sum_{i=1}^{5} \lambda_i g_i \tag{5.11}$$

where λ_i is the Lagrange multiplier corresponding to constraint g_i, $i = 1, \ldots, 5$ as defined in Eqs. (5.6)–(5.10).

Because r_3 and r_4 are less significant than r_1 and r_2 (Section 3.2), the transversality conditions are complete (more than 30 sections each) if we consider r_1 to r_4.To simplify the analysis, we ignore r_3 and r_4. In addition, because Eqs. (5.9) and (5.10) and the equations of $\frac{d\overline{IFF(t)}}{dt}$ and $\frac{dS_{switch}(t)}{dt}$ have correlations with each other, $\frac{d\overline{IFF(t)}}{dt}$ can be substituted into $\frac{dS_{switch}(t)}{dt}$:

$$\frac{dS_{switch}(t)}{dt} = \frac{f\left(\overline{IFF(t)}\right)\left(1+\exp\left(\overline{IFF(t)}\right)\right)^2 + r_1 S(t)\exp\left(\overline{IFF(t)}\right)}{\left(1+\exp\left(\overline{IFF(t)}\right)\right)^2 - r_2 S(t)\exp\left(\overline{IFF(t)}\right)} \frac{dS(t)}{dt} \tag{5.12}$$

and then

$$\frac{d\overline{IFF(t)}}{dt} = \frac{\left(1+\exp\left(\overline{IFF(t)}\right)\right)^2\left(r_1 + r_2 f\left(\overline{IFF(t)}\right)\right)}{\left(1+\exp\left(\overline{IFF(t)}\right)\right)^2 - r_2 S(t)\exp\left(\overline{IFF(t)}\right)} \frac{dS(t)}{dt} \tag{5.13}$$

Also, we substitute $N(t) = S(t) + I(t) + R(t)$ into Eq. (5.6). In the Hamiltonian function (5.11), the constraint functions g_i, $i = 1, \ldots, 5$, are defined as

$$g_1 = \frac{dS(t)}{dt} = \mu I(t) + \mu R(t) + \beta_b u S_{switch}(t) - \beta_b S(t) \tag{5.14}$$

$$g_2 = \frac{dI(t)}{dt} = \beta_b S(t) - \beta_b u S_{switch}(t) - \mu I(t) - \gamma I(t) \tag{5.15}$$

$$g_3 = \frac{dR(t)}{dt} = \gamma I(t) - \mu R(t) \tag{5.16}$$

$$g_4 = \frac{dS_{switch}(t)}{dt} = \frac{f\left(\overline{IFF(t)}\right)\left(1+\exp\left(\overline{IFF(t)}\right)\right)^2 + r_1 S(t)\exp\left(\overline{IFF(t)}\right)}{\left(1+\exp\left(\overline{IFF(t)}\right)\right)^2 - r_2 S(t)\exp\left(\overline{IFF(t)}\right)} \frac{dS(t)}{dt} \tag{5.17}$$

$$g_5 = \frac{d\overline{IFF(t)}}{dt} = \frac{\left(1+\exp\left(\overline{IFF(t)}\right)\right)^2\left(r_1 + r_2 f\left(\overline{IFF(t)}\right)\right)}{\left(1+\exp\left(\overline{IFF(t)}\right)\right)^2 - r_2 S(t)\exp\left(\overline{IFF(t)}\right)} \frac{dS(t)}{dt} \tag{5.18}$$

Application of the Pontryagins maximum principle and the optimal control theory from [44] achieved the following theorem.

Theorem 4. *Let $S(t)$, $I(t)$, $R(t)$, $S_{switch}(t)$, and $\overline{IFF(t)}$ be optimal state solutions with associated optimal control variable $u(t)$ for the optimal control problem. Then adjoint (auxiliary) variables $\lambda_1(t)$, $\lambda_2(t)$, $\lambda_3(t)$, $\lambda_4(t), \lambda_5(t)$ satisfy*

$$\frac{\partial \lambda_1}{\partial t} = -\frac{\partial H}{\partial S} \tag{5.19}$$

$$\frac{\partial \lambda_2}{\partial t} = -\frac{\partial H}{\partial I} \tag{5.20}$$

$$\frac{\partial \lambda_3}{\partial t} = -\frac{\partial H}{\partial R} \tag{5.21}$$

$$\frac{\partial \lambda_4}{\partial t} = -\frac{\partial H}{\partial S_{switch}} \tag{5.22}$$

$$\frac{\partial \lambda_5}{\partial t} = -\frac{\partial H}{\partial \overline{IFF}} \tag{5.23}$$

with transversality conditions as

$$\lambda_i(t_f) = 0 \ (i = 1,\ 2,\ 3,\ 4,\ 5) \tag{5.24}$$

where t_f is the final time of the control.

Proof. Based on the Pontryagins maximum principle [44], given the fundamental system of equations

$$\frac{dx^i}{dt} = g_i(x, u) \ (i = 1,\ 2,\ 3,\ 4,\ 5) \tag{5.25}$$

and another system of equations in auxiliary variables λ_1, $\lambda_2, \lambda_3, \lambda_4, \lambda_5$

$$\frac{d\lambda_i}{dt} = -\sum_{i=1}^{5} \frac{\partial g_i(x(t), u(t))}{\partial x^i} \lambda_i \ (i = 1,\ 2,\ 3,\ 4,\ 5) \tag{5.26}$$

then, in the IFF-SIR model, auxiliary variables λ_i are independent from state variables such as $S(t), I(t), R(t),\ S_{switch}(t)$ and $\overline{IFF(t)}$:

$$\frac{d\lambda_i}{dt} = -\sum_{i=1}^{5} \frac{\partial g_i}{\partial x^i}\lambda_i - \sum_{i=1}^{5} \frac{\partial \lambda_i g_i}{\partial x^i} = -\frac{\partial \sum \lambda_i g_i}{\partial x^i} \tag{5.27}$$

In addition, $F(I)$ and $F(S_{switch})$ are independent from state variables:

$$\frac{d\lambda_i}{dt} = -\frac{\partial \sum \lambda_i g_i}{\partial x^i} = -\frac{\partial\ (F(I) + F(S_{switch}) + \sum \lambda_i g_i)}{\partial x^i} \tag{5.28}$$

Then

$$\frac{d\lambda_i}{dt} = -\frac{\partial H}{\partial x^i} \tag{5.29}$$

where x^i includes $S(t), I(t), R(t),\ S_{switch}(t)$ and $\overline{IFF(t)}$.

5.4. Existence of an optimal control

Theorem 7. *Let $S(t), I(t), R(t), S_{switch}(t)$ and $\overline{IFF(t)}$ be control states with associated control variable $u(t)$ for the optimal control problem. Then unique optimal control $u^*(t)$ minimizes the Hamiltonian function H:*

$$\frac{\partial H}{\partial u} = 2b_1(u^* - 1 + b_2)S_{switch} + \lambda_1 \beta_b S_{switch} - \lambda_2 \beta_b S_{switch} = 0 \tag{5.30}$$

Proof. The Hamiltonian function H can be normalized as

$$H = \alpha u^2 + \beta u + \gamma \tag{5.31}$$

where $\alpha \geq 0$ and β and γ are independent from u because the only quadratic term of u of H comes from

$$F(S_{switch}(t)) = b_1(1 - u - b_2)^2 S_{switch}(t) \tag{5.32}$$

Since $S_{switch} \geq 0$, then $\alpha = b_1 * S_{switch} \geq 0$, and the Hamiltonian function H has a global minimization at $u = -\frac{\beta}{2\alpha}$, meaning that the interval $u \in [0, 1]$ contains only one optimal control u^* that can minimize H, whether or not the interval $u \in [0, 1]$ contains $u = -\frac{\beta}{2\alpha}$.

In addition, the integrand of the objective function given by the Hamiltonian function H is convex in the control strategy set u, which is also convex and closed by definition. Conditions for the existence of optimal controls are satisfied because the model is linear in the control variables and bounded by a linear system in the state variables [43].

Then the final solution of the optimal control problem is

$$u^*(t) = \min\left\{\max\left(0; \frac{\beta_b(\lambda_2(t) - \lambda_1(t)) - b_2 + 1}{2b_1}\right); 1\right\} \tag{5.33}$$

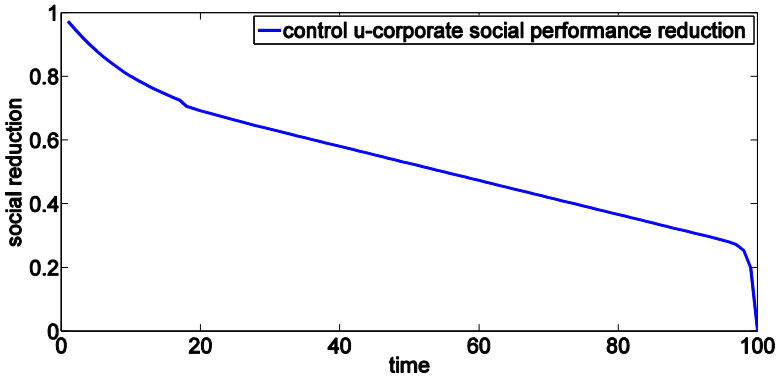

Fig. 11. Optimal corporates with reduced social performance.

5.5. Numerical simulations

This section provides numerical simulation to illustrate our research. Based on the final solution in Eq. (5.33), $u^*(t)$ depends on $\lambda_1(t)$, $\lambda_2(t), \lambda_3(t), \lambda_4(t), \lambda_5(t)$. For the sake of simplicity, we use f to represent $f(\overline{IFF(t)})$ in the following process. We calculate the necessary conditions for $\lambda_1(t)$, $\lambda_2(t), \lambda_3(t), \lambda_4(t), \lambda_5(t)$ as

$$\begin{aligned}\frac{\partial \lambda_1}{\partial t} &= -\frac{\partial H}{\partial S} = (\lambda_1-\lambda_2)\beta_b - -\frac{\exp\left(\overline{IFF(t)}\right)\left(1+\exp\left(\overline{IFF(t)}\right)\right)^2}{\gamma^2} \\ &\quad *(\mu I+\mu R+\beta_b u S_{switch}-\beta_b S)* \\ &\quad \left(\lambda_4 r_1-\lambda_4 r_2 f-\lambda_5 r_1 r_2-\lambda_5 {r_2}^2 f\right) \\ &\quad +\frac{\beta_b\lambda_4\left(f\left(1+\exp\left(\overline{IFF(t)}\right)\right)^2+r_1 S\exp\left(\overline{IFF(t)}\right)\right)}{\gamma} \end{aligned} \tag{5.34}$$

$$\frac{\partial \lambda_2}{\partial t} = -\frac{\partial H}{\partial I} = -z+(\lambda_2-\lambda_1)\mu+(\lambda_2-\lambda_3)\gamma-\frac{\mu}{\gamma}*\phi \tag{5.35}$$

$$\frac{\partial \lambda_3}{\partial t} = -\frac{\partial H}{\partial R} = (\lambda_3-\lambda_1)\mu-\frac{\mu}{\gamma}*\phi \tag{5.36}$$

$$\frac{\partial \lambda_4}{\partial t} = -\frac{\partial H}{\partial S_{switch}} = (\lambda_2-\lambda_1)\beta_b u-\frac{\beta_b u}{\gamma}\phi \tag{5.37}$$

$$\begin{aligned}\frac{\partial \lambda_5}{\partial t} &= -\frac{\partial H}{\partial \overline{IFF}} = -\frac{(\mu I+\mu R+\beta_b u S_{switch}-\beta_b S)\exp\left(\overline{IFF(t)}\right)}{\gamma^2} \\ &\quad *\{\lambda_5 r_2 S\left(1+\exp\left(\overline{IFF(t)}\right)\right)(r_1+r_2 f)\left(1+3\exp\left(\overline{IFF(t)}\right)\right) \\ &\quad +\lambda_5 r_2\left(1+2\exp\left(\overline{IFF(t)}\right)\right)\left[\left(1+\exp\left(\overline{IFF(t)}\right)\right)^2+S\exp\left(\overline{IFF(t)}\right)\right] \\ &\quad +\lambda_4\left(1+\exp\left(\overline{IFF(t)}\right)\right)^2[1+2\exp\left(\overline{IFF(t)}\right)+r_1 S \\ &\quad +r_2 Sf]-\lambda_4\left(1+\exp\left(\overline{IFF(t)}\right)\right)\exp\left(\overline{IFF(t)}\right)(2r_2 Sf-2r_1 S) \\ &\quad +\lambda_4(1+2\exp\left(\overline{IFF(t)}\right))\exp\left(\overline{IFF(t)}\right)r_2 S\} \end{aligned} \tag{5.38}$$

where

$$\nu = \left(1+\exp\left(\overline{IFF(t)}\right)\right)^2-r_2 S\exp\left(\overline{IFF(t)}\right) \tag{5.39}$$

$$\phi = \left((\lambda_4 f+\lambda_5 r_1+\lambda_5 r_2 f)\left(1+\exp\left(\overline{IFF(t)}\right)\right)^2+\lambda_4 r_1 S\exp\left(\overline{IFF(t)}\right)\right) \tag{5.40}$$

Using the IFF-SIR dynamic system with control in Eq. (5.3), the boundary constraints in Eqs. (5.19)–(5.23), and final solution (5.32), we calculate $u^*(t)$ by iteration algorithm [39] according to the following steps:

Step 1: Order a constant control in the first iteration ($j=1$). We choose the maximum number of control $u(t)$ as this constant in order to simplify the problem.

$$u_1(t) = 1$$

Step 2: Using the IFF-SIR dynamic system expression, calculate $(S_j(t), I_j(t), R_j(t), S_{switch\,j}(t), \overline{IFF_j(t)})$ in the jth iteration.

Step 3: Based on the boundary constraints expression, calculate $\lambda_{i,j}(t)$ using transversality conditions as initial conditions.

Step 4: Calculate $u_j{}^*(t)$ by the final solution of the optimal control problem. We use a convex combination to calculate $u_{j+1}(t)$.

Step 5: Repeat steps 2, 3, and 4 to obtain the numerical optimal control solution $u^*(t) = u_j(t)$ until terminal condition

$$u_j(t) = u_{j+1}(t)$$

In order to verify validity of the optimal control, a simulation run compares results of the model with and without control using the iteration algorithm. Assuming that the total number of individuals in the global contact network is $N = 1000$: 980 susceptible, 20 infected, 0 recover and 300 switch individuals, let $z = 2000$ [45] and $b_1 = 60$ [46]. When $u = 0$, the financial loss is zero and $b_2 = 1$. We observe the trend of individuals in each state and the estimated $\overline{IFF(t)}$ based on the regression relationship over the 100-day period. Observations throughout five replications revealed that the terminating condition was almost satisfied ($|u_j(t) - u_{j+1}(t)| \le 0.001$) after the 15^{th}th iteration, which means the iteration result satisfied the terminal condition at Step 5 of the iteration algorithm. Overall, the optimal corporate social performance reduction decreased through the time line, as shown in Fig. 11. The optimal solution at the onset of a disease epidemic is to reduce almost all corporate social performance. The optimal solution at the last phase of a disease suggests that people choose normal behavior.

In order to verify validity of the optimal control, we compare simulation results (total infections and total susceptive switch populations) of the IFF-SIR model with control and without control to various initial settings. We compare the simulations with initial population $N = 1000$ ($S = 980; I = 20; R = 0; S_{switch} = 50$), $N = 1000$ ($S = 960; I = 40; R = 0; S_{switch} = 50$), $N = 1000$ ($S = 940; I = 60; R = 0; S_{switch} = 50$), and $N = 1000$ ($S = 920; I = 80; R = 0; S_{switch} = 50$). Although the tendencies are similar, as shown in Fig. 12, the IFF-SIR model with control has less total infectious and less total susceptive switch population. Therefore, the optimal control policy successfully reduces the financial loss of infections. Results also showed that the switch level in the IFF-SIR model with control is not a constant, suggesting that reduction of social performance is sensitive to epidemic change, leading to the conclusion that the optimal control solution reduces unnecessary financial loss in the epidemic.

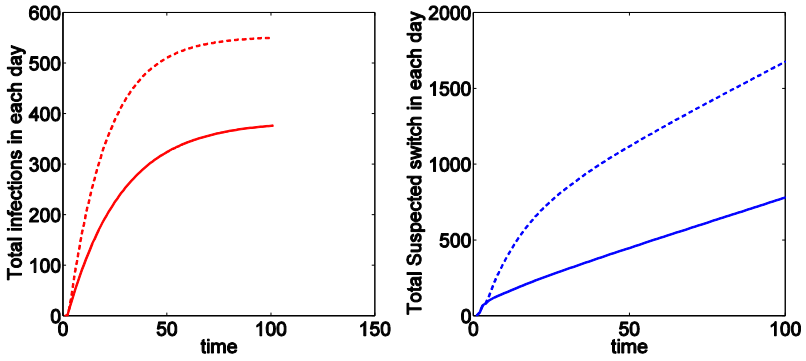

(a) With initial population $N = 1000$ (S = 980; I = 20; R = 0; $S_{switch} = 50$)

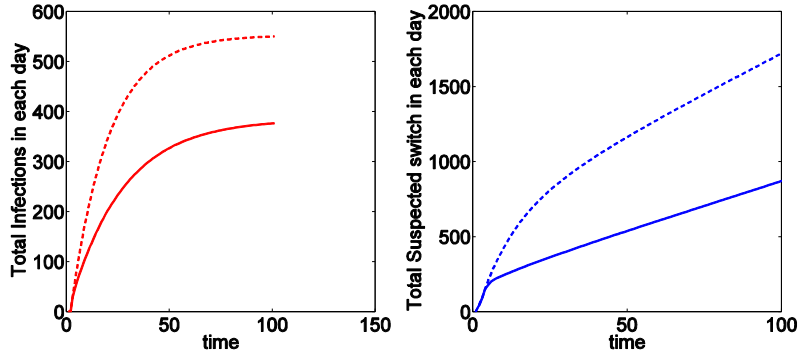

(b) With initial population $N = 1000$ (S = 960; I = 40; R = 0; $S_{switch} = 50$)

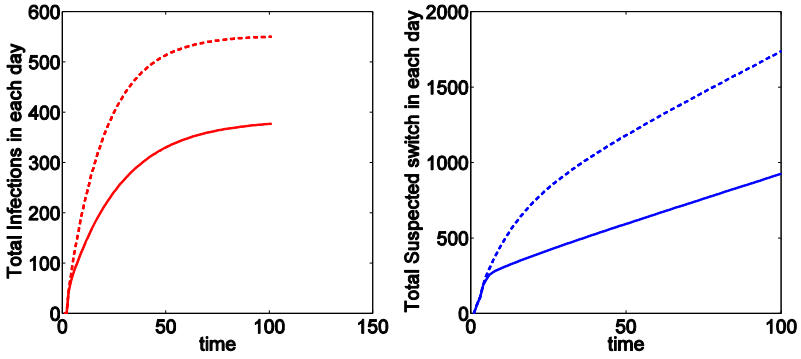

(c) With initial population $N = 1000$ (S = 940; I = 60; R = 0; $S_{switch} = 50$)

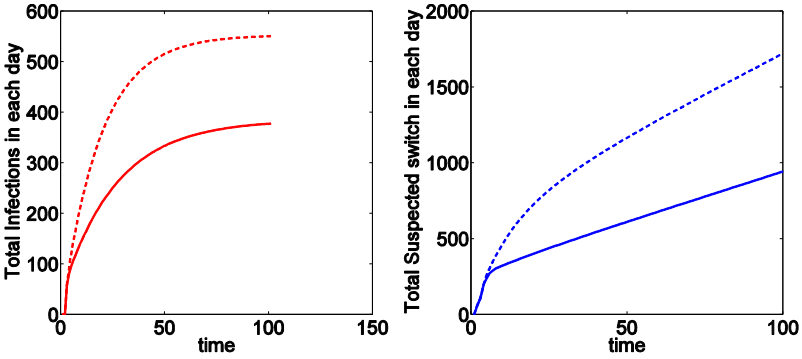

(d) With initial population $N = 1000$ (S = 920; I = 80; R = 0; $S_{switch} = 50$)

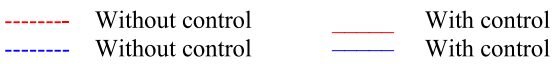

Fig. 12. Comparison of the IFF-SIR model with and without control in four numerical simulations.

6. Summary and discussion

This paper synthesized local and global contact networks and perceptual and rational information to develop an IFF model to define the fear factor for susceptible individuals in order to determine how information affects emotion or opinion, thereby altering individuals' behavior during an epidemic. Moreover, this paper first attempted to explain how an individual's emotions and perceptions on the current information influence their switching behavior using a mathematical model. So this research can be utilized to study the complex emotion and behavior changes during disease outbreaks. Following stability analysis, we identified and proved four necessary conditions of IFF stability in order to better understand the role of IFF in epidemic transmission within the individual model. Regression analysis was used to average IFF among all susceptible individuals, revealing a statistically significant regression relationship between $\overline{IFF(t)}$ and $S(t), I(t), R(t), S_{switch}(t)$. Then we introduced an IFF-SIR dynamic system that includes differential equations of $S(t)$, $I(t)$, $R(t)$, $S_{switch}(t)$, and $\overline{IFF(t)}$. Using the Lyapunov stability theory, we found that IFF-SIR has infinite stability points. Finally, we defined financial loss as the objective function in the optimal control problem, and we proposed the optimal suggestion for reduction of social performance throughout an epidemic. Although regression analysis allows us to research IFF in disease transmission, the feasible range of population is limited by data. Therefore, future studies should include real data collection and use a multilayer method to divide a population.

References

[1] Funk S, Marcel S, Vincent AAJ. Modelling the influence of human behaviour on the spread of infectious diseases: a review. J R Soc Interface 2010;7:1247–56.
[2] Polgar S. Health and human behavior: areas of interest common to the social and medical sciences. Curr Anthropol 1962;3(2):159–205.
[3] Morse SS. Factors in the emergence of infectious diseases. In: Plagues and politics. UK: Palgrave Macmillan; 2001. p. 8–26.
[4] Cohen ML. Changing patterns of infectious disease. Nature 2000;406(6797):762–7.
[5] Lemerise EA, Arsenio WF. An integrated model of emotion processes and cognition in social information processing. Child Dev 2000;71(1):107–18.
[6] Dunn JR, Schweitzer ME. Feeling and believing: the influence of emotion on trust. J Personal Soc Psychol 2005;88(5):736.
[7] Griskevicius V, Shiota MN, Neufeld SL. Influence of different positive emotions on persuasion processing: a functional evolutionary approach. Emotion 2010;10(2):190.
[8] Zhao S, Kuang Y, Ben-Arieh D. Information dissemination and human behaviors in epidemics. In: Proceedings of IIE annual conference. Institute of Industrial Engineers; 2015. 1907
[9] Johnston AC, Warkentin M. Fear appeals and information security behaviors: an empirical study. MIS Q 2010;34:549–66.
[10] Geer JH. The development of a scale to measure fear. Behav Res Therapy 1965;3(1):45–53.
[11] Funk S, Gilad E, Watkins C, Jansen VA. The spread of awareness and its impact on epidemic outbreaks. Proc Natl Acad Sci 2009;106(16):6872–7.
[12] Newman ME. Spread of epidemic disease on networks. Phys Rev E 2002;66(1):016128.
[13] Tien JH, Earn DJ. Multiple transmission pathways and disease dynamics in a waterborne pathogen model. Bull Math Biol 2010;72(6):1506–33.
[14] Korobeinikov A. Lyapunov functions and global stability for SIR and SIRS epidemiological models with non-linear transmission. Bull Math Biol 2006;68(3):615–26.
[15] Parkinson B. Interpersonal emotion transfer: contagion and social appraisal. Soc Personal Psychol Compass 2011;5(7):428–39.
[16] Epstein JM, Parker J, Cummings D, Hammond RA. Coupled contagion dynamics of fear and disease: mathematical and computational explorations. PLoS One 2008;3(12):e3955.
[17] Chen FH. Modeling the effect of information quality on risk behavior change and the transmission of infectious diseases. Math Biosci 2009;217(2):125–33.
[18] Hogg MA, Reid SA. Social identity, self-categorization, and the communication of group norms. Commun Theory 2006;16(1):7–30.
[19] Wöllmer M, Eyben F, Reiter S, Schuller B, Cox C, Douglas-Cowie E. Abandoning emotion classes-towards continuous emotion recognition with modelling of long-range dependencies. In: Proceedings of INTERSPEECH, 2008; 2008. p. 597–600.
[20] Gunes, H., 2010. Automatic, dimensional and continuous emotion recognition.
[21] Suls J, Green P, Hillis S. Emotional reactivity to everyday problems, affective inertia, and neuroticism. Personal Soc Psychol Bull 1998;24(2):127–36.
[22] Ebner-Priemer UW, Eid M, Kleindienst N, Stabenow S, Trull TJ. Analytic strategies for understanding affective (in) stability and other dynamic processes in psychopathology. J Abnorm Psychol 2009;118(1):195.
[23] Jahng S, Wood PK, Trull TJ. Analysis of affective instability in ecological momentary assessment: Indices using successive difference and group comparison via multilevel modeling. Psychol Methods 2008;13(4):354.
[24] Trull TJ, Solhan MB, Tragesser SL, Jahng S, Wood PK, Piasecki TM. Affective instability: measuring a core feature of borderline personality disorder with ecological momentary assessment. J Abnorm Psychol 2008;117(3):647.
[25] Zhao S, Wu J, Ben-Arieh D. Modeling infection spread and behavioral change using spatial games. Health Syst 2015;4(1):41–53.
[26] Steimer T. The biology of fear-and anxiety-related behaviors. Dialogues in Clin Neurosci 2002;4:231–50.
[27] McEwen BS. Physiology and neurobiology of stress and adaptation: central role of the brain. Physiol Rev 2007;87(3):873–904.
[28] Baker GA. Food safety and fear: Factors affecting consumer response to food safety risk. Int Food Agribus Manag Rev 2003;6(1):1–11.
[29] Scoglio CM, Bosca C, Riad MH, Sahneh FD, Britch SC, Cohnstaedt LW. Biologically informed individual-based network model for Rift Valley fever in the US and evaluation of mitigation strategies. PLoS One 2016;11(9):e0162759.
[30] Meyers L. Contact network epidemiology: Bond percolation applied to infectious disease prediction and control. Bull Am Math Soc 2007;44(1):63–86.
[31] Sahneh FD, Scoglio C. Competitive epidemic spreading over arbitrary multilayer networks. Phys Rev E 2014;89(6):062817.
[32] Poli R, Kennedy J, Blackwell T. Particle swarm optimization. Swarm Intell 2007;1(1):33–57.
[33] Bandura A. Social cognitive theory of mass communication. Media Psychol 2001;3(3):265–99.
[34] Lo AW, Repin DV, Steenbarger BN. Fear and greed in financial markets: a clinical study of day-traders. National Bureau of Economic Research; 2005. (No. w11243).
[35] Das E, Fennis BM. In the mood to face the facts: when a positive mood promotes systematic processing of self-threatening information. Motiv Emot 2008;32(3):221–30.
[36] Shakeri H, Sahneh FD, Scoglio C, Poggi-Corradini P, Preciado VM. Optimal information dissemination strategy to promote preventive behaviours in multilayer epidemic networks. Math Biosci Eng 2015;12(3):609–23.
[37] Eberhart R, Shi Y. Particle swarm optimization: developments, applications and resources. In: Proceedings of the 2001 congress on evolutionary computation, 1. IEEE; 2001. p. 81–6.
[38] Emvudu Y, Demasse R, Djeudeu D. Optimal control of the lost to follow up in a tuberculosis model. Comput Math Methods Med 2011;2011:12.
[39] Neyman J, Pearson ES. The testing of statistical hypotheses in relation to probabilities a priori. In: Mathematical proceedings of the Cambridge philosophical society, 29. Cambridge University Press; 1933. p. 492–510.
[40] Lyapunov AM. The general problem of the stability of motion. Int J Control 1992;55(3):531–4.
[41] Van Den Bergh F. An analysis of particle swarm optimizers. University of Pretoria; 2006. Doctoral dissertation.
[42] Ruf BM, Muralidhar K, Brown RM, Janney JJ, Paul K. An empirical investigation of the relationship between change in corporate social performance and financial performance: a stakeholder theory perspective. J Bus Ethics 2001;32(2):143–56.
[43] Brammer S, Millington A. Does it pay to be different? An analysis of the relationship between corporate social and financial performance. Strateg Manag J 2008;29(12):1325–43.
[44] Pontryagin LS. Mathematical theory of optimal processes. CRC Press; 1987.
[45] Greco DB, Simao M. Brazilian policy of universal access to AIDS treatment: sustainability challenges and perspectives. AIDS 2007;21:S37–45.
[46] Renneboog L, Ter Horst J, Zhang C. Socially responsible investments: institutional aspects, performance, and investor behavior. J Bank Financ 2008;32(9):1723–42.